VYSOKÉ UČENÍ TECHNICKÉ V BRNĚ

Fakulta elektrotechniky a komunikačních technologií

Ústav radioelektroniky

Ing. Mgr. Zdeněk Tobeš

**ANALOG NEURAL NETWORKS FOR
THE CONTROL OF ADAPTIVE ANTENNAS**

**ANALOGOVÉ NEURONOVÉ SÍTĚ PRO ŘÍZENÍ
ADAPTIVNÍCH ANTÉN**

SHORT VERSION OF PHD THESIS

Obor: Elektronika, měřící a sdělovací technika

Školitel: Doc. Dr. Ing. Zbyněk Raida

Oponenti: Prof. Ing. Dalibor Biolek, CSc.
       Prof. Ing. Stanislav Marchevský, CSc.

Datum obhajoby: 21. 6. 2002

KLÍČOVÁ SLOVA

Adaptivní anténa, váhový vektor, gradientní algoritmus, Kalmanův filtr, analogový neuron, Wangova analogová neuronová sít, Kalmanova analogová neuronová síť, reálný operační zesilovač, poměr vlastních čísel matice vstupního signálu, konvergenční vlastnosti

KEY WORDS

Adaptive antenna, weight vector, gradient algorithm, Kalman filter, analog neuron, analog neural network of Wang, analog neural network of Kalman, real operational amplifier, ratio of eigenvalues of the input signal matrix, convergence properties

MÍSTO ULOŽENÍ PRÁCE:

Vědecké oddělení FEKT VUT v Brně

CONTENTS

ABSTRAKT

Disertační práce se zabývá vývojem rychlých a stabilních řídicích systémů adaptivních antén, založených na analogových neuronových sítích. Její první část obsahuje úvod do problematiky adaptivních antén a přehled dosavadních přístupů k řízení adaptivních antén. Ve druhé části jsou diskutovány jednotlivé druhy analogových neuronových sítí, největší pozornost je věnována tzv. Wangovým a Kalmanovým neuronovým sítím, které jsou v této části disertační práce matematicky analyzovány a jsou zde navrženy jejich modifikace, vedoucí k podstatnému zlepšení konvergenčních vlastností těchto sítí. Třetí část práce se zabývá aplikací těchto analogových neuronových sítí a jejich modifikací v řídicích systémech adaptivních antén.

Cílem druhé části disertační práce je vyřešit dva hlavní problémy doposud používaných analogových neuronových sítí - nízkou rychlost konvergence a její velkou závislost na poměru vlastních čísel matice vstupního signálu. Za tímto účelem zde byly podrobně analyzovány konvergenční vlastnosti původních verzí těchto sítí a vliv jednotlivých obvodových prvků na tyto vlastnosti, zejména vliv reálných operačních zesilovačů. V případě Wangovy sítě byla provedena matematická analýza s makromodelem operačního zesilovače, popisujícím jeho lineární i nelineární vlastnosti. Na základě výsledků těchto analýz byly navrženy modifikace jednotlivých stavebních prvků diskutovaných analogových neuronových sítí, vedoucí ke zlepšení jejich konvergenčních vlastností. V případě Kalmanovy neuronové sítě bylo dosaženo zlepšení rychlosti konvergence cca o tři řády vůči původní verzi této sítě a velmi malé závislosti rychlosti konvergence na poměru vlastních čísel matice vstupního signálu. Velký vliv na dosažení těchto výsledků měla modifikace Kalmanovy sítě, spočívající ve filtraci signálu Kalmanova zisku. Pozornost byla věnována převážně neuronovým sítím pro řešení soustavy reálných lineárních rovnic, diskutovány však byly i neuronové sítě sloužící k řešení problému minimalizace kvadratické funkce, omezené lineární podmínkou.

Třetí část dizertační práce se zabývá aplikací analogových neuronových sítí v řídicích systémech adaptivních antén. Na základě výsledků získaných ve druhé kapitole jsou zde navrženy řídicí systémy adaptivních antén, založené na původní Wangově a Kalmanově neuronové síti a na modifikované Kalmanově síti. Konvergenční vlastnosti těchto řídicích systémů byly zkoumány prostřednictvím počítačových simulací, takto byly zjištěny konvergenční vlastnosti velmi podobné výchozím obecným neuronovým sítím. Ve srovnání s ostatními diskutovanými řídicími systémy vykazuje řídicí systém založený na modifikované Kalmanově síti velmi dobré konvergenční vlastnosti, které vyhovují požadavkům na provoz adaptivní antény v reálném čase.

4

1   INTRODUCTION

1.1 PROBLEM FORMULATION

An adaptive antenna array is an antenna system, which automatically sets minims of its directivity pattern to directions from which the most powerful interference signals come. Also, an adaptive antenna can be understood as a spatial filter, which does not attenuate desired signals arriving from the main lobe direction and which adaptively suppresses signals arriving from other directions.

From the optimization point of view, adaptive antennas are parallel systems, which are asked to be very fast in many applications. Since digital processors work in a sequential way and since parallel multiprocessor systems are extremely expensive, analog parallel processors seem to be a very suitable alternative for the control of an optimization process. Unfortunately, most of the so far developed analog processors suffer from non-stability, low convergence rate and sensitivity to setting of adaptation parameters.

The discovered problems form the kernel of the presented dissertation thesis.

1.2 TODAY'S STATE OF SOLVING PROBLEM

At the present time, the most adaptive antennas are based on the pilot signal method [1] and the steering vector method [2].

In the case of the pilot signal, a transmitter transmits a signal, which is known at the receiving side during the learning period. Therefore, an error signal, which equals to the difference between the desired pilot signal and the actual signal at the antenna output, can be defined and the mean squared error can be minimized to obtain an optimal signal to interference ratio at the antenna output.

In the case of the steering vector, the mean power of the signal at the antenna output is minimized. If the minimization is constrained in order not to influence parameters of the antenna system in the main lobe direction (from which a desired signal come), then the minimization reduces interference signals only and the signal to interference ratio at the antenna output is optimized again.

Both the methods yield the set of simultaneous linear equations, which has to be solved in real time in order to synthesize the proper directivity pattern. The matrix of coefficients is auto- or cross-correlation matrix of signals at the outputs of antenna elements, unknown column vector contains complex weights of antenna elements, and zeros and ones form the right-hand side vector. Today, the described matrix equation is solved by the following methods.

1.2.1   Correlation loop

The correlation loop was the first analog solver for the steering vector system, which is called the side-lobe canceller [3]. The side-lobe canceller consists of a main antenna, which is accompanied by an auxiliary omni-directional antenna in order to to create a null in the side-lobes of the combined pattern of this antenna system. The

mean power of interference signals is minimized and signal to interference ratio is optimized at the antenna output [8].
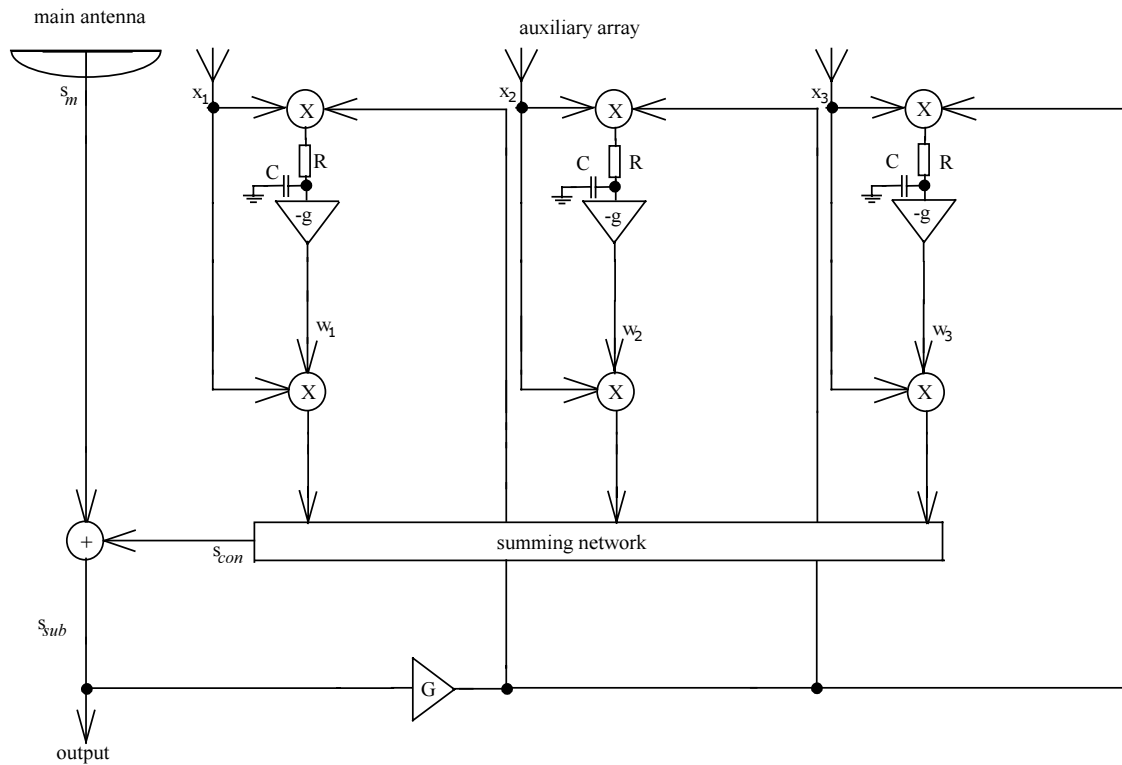

Fig. 1.1: The standard LMS array in a side-lobe canceller configuration

For suppressing of more as one interference signal only, the mentioned adaptive antenna was generalized by the superposition of N auxiliary antennas, completed by N correlation loops [8]. Since N auxiliary elements can produce N independent beams, the system can generally deal with up to N interference signals.

Unfortunately, the described adaptive control exhibits following main disadvantages [3], [8]:

Since minimizing output power residue is unconstrained in a fact, the adaptive process can also minimize desired signals, because the process can distinguish desired signal from clutter or interference only on the basis of power and energy.

The power level at the antenna element determines loop voltage gain and speed in canceling the interference signal. Steady-state cancellation of extended clutter or interference depends on their power. Transient cancellation of short target signals depends on both power and duration, or on total energy. Adaptive system can work only when extended clutter and interference signal show considerably more duration and energy than discrete target signal, which might be screen.

The gain of the adaptive mode (which is individual loop gain times number of loops) must be set in order to produce only minor cancellation of the strongest desired main lobe signal, and to provide reasonable cancellation and settling times of the undesired sources.

Due to the above listed disadvantages of the described analog adaptation processors, more sophisticated adaptation algorithms were worked up as it is going to be described in the following paragraphs.

1.2.2 LMS algorithm and its improved versions

There is a number of algorithms minimizing the mean squared error. The minimization is usually reached by gradient-searching techniques, which are based on changing the weighting vector in the contra-direction of an estimate of the gradient of the mean squared error with respect to weights [1]

$$\frac{d\mathbf{W}(t)}{dt} = -k_s \nabla \varepsilon^2 .$$ (1.1)

Here, $\mathbf{W}(t)$ is the weighting vector, k_s is a positive scalar constant controlling rate of convergence and stability of the algorithm, and $\nabla \varepsilon^2$ is an estimate of the gradient of the mean squared error with respect to weights.
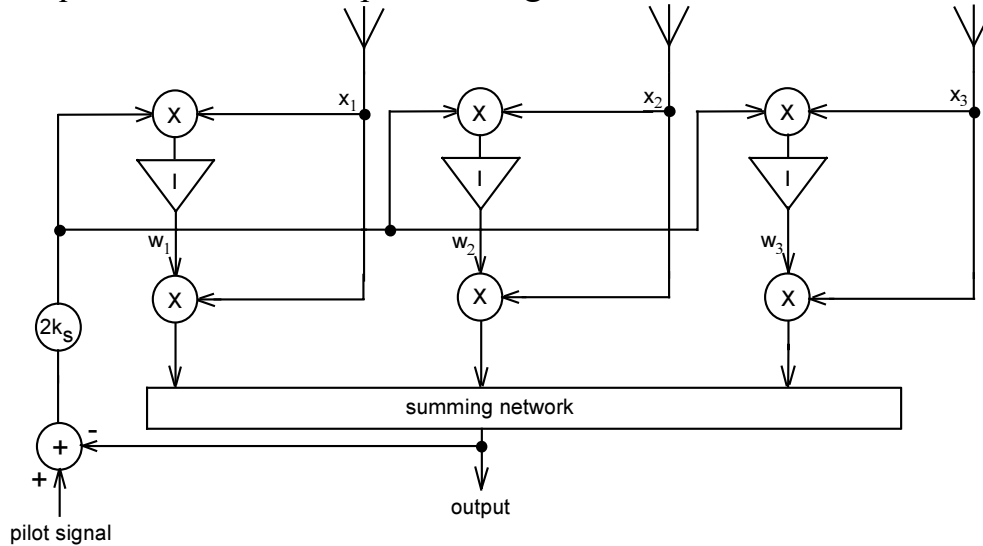

Fig. 1.2: The pilot-signal-based adaptive antenna controlled by the LMS algorithm

Adaptive algorithms differ in the way, how the gradient of the mean squared error is estimated. Considering Least Mean Square (LMS) algorithm [1], the squared-error mean value is replaced by the instant one. The main disadvantages of the classical analog LMS algorithm are especially low convergence rate and its dependency on the adaptive parameters. Therefore, a lot of various versions of this algorithm have been worked up, [9] – [11] e.g.

The adaptive antenna, controlled by LMS algorithm, is depicted in Fig. 1.2. Investigating the time course of the circuit in Fig. 1.1, it can be expressed as [10]

$$\frac{d\mathbf{W}(t)}{dt} = -\frac{1}{T}[\mathbf{I} + gG\mathbf{X}(t)\mathbf{X}^{\mathrm{H}}(t)]\mathbf{W}(t) - \frac{gG}{T}\mathbf{X}(t)s_m^*(t) .$$ (1.2)

Here, $T=RC$ is the open-loop time constant of the first-order LMS loop, and - gG is the negative feedback gain. Rearranging the relation (1.2) and replacing the term

$\mathbf{X}(t)s_m{}^*(t)$ by its average value S yields a relation for computing the optimal average weighting vector $\mathbf{W}_{opt}$ for $gG \gg 1$ [10]

$$\{\mathbf{W}(t)\} = -gG(\mathbf{I} - \exp[-t(\mathbf{I} + gG\mathbf{R})/T])(\mathbf{I} + gG\mathbf{R})^{-1}\mathbf{S} +$$
$$+ \exp[-t(\mathbf{I} + gG\mathbf{R})/T]\mathbf{W}(0). \tag{1.3}$$

The closed loop time constants of this algorithm can be obtained from the diagonalized auto-correlation matrix $\mathbf{R} = \mathbf{E}\Lambda\mathbf{E}^{\mathrm{H}}$, where Λ is the diagonal matrix of positive real eigenvalues λ_i of $\mathbf{R}$ and $\mathbf{E}$ is unitary transform matrix ($\mathbf{E}^{\mathrm{H}} = \mathbf{E}^{-1}$), columns of which are the corresponding orthonormal eigenvectors of $\mathbf{R}$ [9], [10]. The averaged equation (1.3) is then diagonalized to obtain the uncoupled modes of $\mathbf{W}(t)$ with time constants given by [10]

$$T_i = T/(1 + gG\lambda_i), \quad i = 1, 2, \ldots N. \tag{1.4}$$

Usually (interference sources are partially correlated; sources have widely different power levels etc.), some eigenvalues λ_i are much more larger than others. Large eigenvalues λ_i make then the weighting coefficients jittery causing large variations in residual output power [9], [10], while the small eigenvalues λ_i take very long time to converge.

Therefore, Compton developed an improvement of the LMS feedback loop for obtaining convergence rate almost independent on eigenvalues of $\mathbf{R}$ [9]. The time-averaging products of input signals ensure a sufficient estimation of the matrix $\mathbf{R}$ in the derivative feedback term, and therefore, the near-cancellation of its eigenvalues in the time constants T_i is permitted [9]. The differential equation describing Fig. 1.1 is changed, using Compton improvement, to [10]

$$(\mathbf{I} + 2kc\mathbf{R})\frac{d\mathbf{W}(t)}{dt} = -2k\mathbf{R}\mathbf{W}(t) - 2k\mathbf{S}, \tag{1.5}$$

and time constants are given by [10]

$$T_i = T(1 + 2kc\lambda_i)/2k\lambda_i, \quad i = 1, 2, \ldots N. \tag{1.6}$$

Here, $2k = gG/T$, T is the integrator open-loop time constant, $c = qT$ and the time constants (1.6) can be re-expressed for large values of q, for which $gGq\lambda_{min} \gg 1$, as [10]

$$T_i = T(1 + gqG\lambda_i)/gG\lambda_i. \tag{1.7}$$

Obviously, the proper setting of integration constants T and gains of feedback loops gG is conditioned by the knowledge of the minimal eigenvalue λ_{min} of the auto-correlation matrix $\mathbf{R}$, which depends on unpredictable signal positions and powers. Therefore, a modification of the Compton's circuit, which does not require the knowledge of λ_{min}, was developed by Klemes [10]. In Klemes circuit, time constants T_i are independent on λ_i, and the gain gG plays no role there.

In the Klemes adaptive processor, a perfect integrator is replaced by a single-pole RC low-pass filter of the time constant $T_2 = C_2 R_2$, and the time averager is replaced by similar filter of the time constant $T_1 = C_1 R_1 \ll T_2$. A subtractor is incorporated in the new loop to generate the time-derivative of the weight.

Analysis of the Klemes circuit leads to the second-order differential equation [10]

$$\frac{d^2\mathbf{W}}{dt^2} + \frac{1}{T_1}[(1 + T_1/T_2)\mathbf{I} + gG\mathbf{X}\mathbf{X}^H]\frac{d\mathbf{W}}{dt} +$$

$$+ \frac{1}{T_1 T_2}[\mathbf{I} + \delta gG\mathbf{X}\mathbf{X}^H]\mathbf{W} = -\frac{\delta gG}{T_1 T_2}\mathbf{X}D^*, \qquad (1.8)$$

where the time arguments of $\mathbf{W}(t)$ and $\mathbf{X}(t)$ were omitted for clarity and $\delta = T_2/(T_2 + T_1)$. T_1 is here assumed being much smaller than T_2. As the result of solving (1.8) for $\mathbf{W}$, the time constants of Klemes modified loop are obtained [10]

$$T_i = T_0(1 + bgG\lambda_i)/(1 + agG\lambda_i), \, i = 1,2,...N. \qquad (1.9)$$

Here, $b = 1 \pm \mu_{max}$ and $a = 1 \pm \eta_{max}$, respectively (these parameters approach one in most cases), T_0 is a dominant open-loop time constant, and the parameters μ_{max} and η_{max} are discussed in [10].

Comparing the standard LMS loop, Compton loop and Klemes loop in terms of time constants of the closed feedback loop, following conclusions can be done:

Convergence properties of the standard LMS algorithm are crucially influenced by the spread of eigenvalues of the auto-correlation matrix of input signals. This influence is reduced by modifications of Compton and Klemes. Unfortunately, their solutions exhibit higher complexity of the control circuitry, and moreover, new parameters, values of which have to be properly guessed, are included into the system. Further, it can be shown that Klemes circuit exhibits relatively high misadjustment in the case of the high ratio of eigenvalues (also when only ideal circuit elements are considered). Moreover, in the published papers [9] and [10], no discussion was devoted to the influence of real parameters of the circuitry to the proper function and to the stability of the system.

The so far described analog adaptive processors exhibit strong parallelism (each antenna element has its own feedback loop) and learning ability (the antenna system learns to maximize signal to interference ratio in the actual electromagnetic environment). Therefore, the described adaptive processors are very close by their nature to the artificial neural networks [12]. On the other hand, analog artificial neural networks seem to be attractive to be used for the control of adaptive antennas.

1.2.3 Aims of the dissertation

On the basis of the above-presented overview of so-far developed analog systems for the control of adaptive antennas, following general conclusions can be done:

In the open literature, no approach to the control of adaptive antennas, which fully explores positive features of analog neural networks, has appeared yet.

In the open literature, no discussion has been devoted to a direct way of preparing input patterns for the analog control neural networks of adaptive antennas (without the use of complicated resistive arrays).

In the so-far development, the elimination of the influence of statistical parameters of input signals to the stability of control circuitry has not been satisfactorily solved yet.

In the so-far development, no attention has been paid to the role of properties of real electronic components to the stability and to the convergence properties of the developed systems yet.

Therefore, the presented dissertation was oriented to reaching of following aims:

Since the control of adaptive antennas can be converted to the solution of the set of simultaneous linear equations, various types of analog neural networks, which can be used for this purpose (Wang, Kalman, simplified Kalman and Hopfield) are going to be introduced here and rigorously analyzed. The analysis is oriented towards investigating influence of real electronic components and influence of statistical parameters to the behavior of the system.

Results of the rigorous analysis are going to be used for the development of original modifications of the above mentioned types of neural networks in order to ensure the stability of the system in as wide range of situations as possible.

A special analog circuitry for the direct conversion of antenna signals to input patterns of neural networks is going to be developed. Antenna systems based on the pilot signal and on the steering vector are going to be considered.

2 ANALOG NEURAL NETWORKS

In Chapter 1, two basic methods for steering adaptive antennas were introduced: pilot signal method and steering vector method. Both the methods result in the set of simultaneous linear equations, which have to be solved in real time. In Chapter 1, we have presented several approaches to the iterative solution of the set of equations. The set of N LMS loops (for iterative solution of N equations) can be understood as a recurrent neural network (Wang one), and therefore, we concentrate on solvers of linear equations, which are based on analog neural networks (ANN).

2.1 WANG ANN

In this section, the analog recurrent neural network with the LMS learning algorithm (so called Wang ANN) is reviewed and analyzed. On the basis of discussion of the obtained results, modified versions of Wang ANN are developed.

Wang ANN [13] was designed for the solution of a set of real linear equations

$$\mathbf{A}.\mathbf{v}_s = \mathbf{b}, \qquad (2.1)$$

with the matrix of coefficients $\mathbf{A}$, with the column vector of right-hand sides $\mathbf{b}$, and with the column vector of solutions $\mathbf{v}_s$.

For the matrix $\mathbf{A}$ of the size $N{\times}N$ (2.1), Wang ANN consists of N identical blocks (neurons) connected in parallel (Fig. 2.1).

Operation of Wang ANN can be described as follows: in the beginning of the convergence process, a random vector $\mathbf{v}(0)$ is put into (2.1) instead of the searched solution. If $\mathbf{v}(0)$ is replaced by the vector $\mathbf{v}(t)$, the vector of errors is obtained:

$$\mathbf{e}(t) = \mathbf{b} - \mathbf{A}.\mathbf{v}(t). \qquad (2.2)$$

The squared error vector is minimized by changing $\mathbf{v}(t)$ in the contra-direction of the gradient $\text{grad}_v(\mathbf{e}^2)$ [13]

$$d\mathbf{v}(t)/dt = \eta\mathbf{A}^{\mathrm{T}}\left[\mathbf{b} - \mathbf{A}\mathbf{v}(t)\right] = \theta + \mathbf{W}\mathbf{v}(t), \tag{2.3}$$

where $\theta = \eta\mathbf{A}^{\mathrm{T}}\mathbf{b}$, $\mathbf{W} = -\eta\mathbf{A}^{\mathrm{T}}\mathbf{A}$, $\eta > 0$ is the learning constant.

The elements of the matrix $\mathbf{W}$ are introduced into the neural network in the form of resistors, which are given by the relation

$$R_{i,j} = R_f \big/ |w_{i,j}|. \tag{2.4}$$

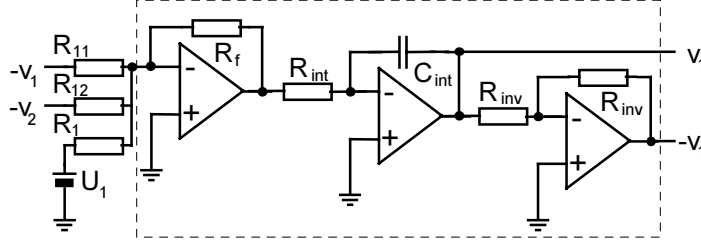Here, R_f denotes the feedback resistor, which is depicted in Fig. 2.1.

Fig. 2.1: The first neuron of one-dimensional Wang neural network

Elements of the column vector θ are introduced into the network by voltage sources U_i and resistors R_i (see Fig. 2.1), which are related by the expression

$$R_f U_i / R_i = \theta_i. \tag{2.5}$$

Then, the neuron consists of the summing amplifier, of the integrator producing v_i, and of the inverter implementing negative elements of the matrix $\mathbf{W}$.

Convergence process of one-dimensional Wang ANN can be described by

$$v_1(p) = R_f\left(\frac{U_1}{pR_1} - \frac{v_1}{R_{11}}\right)\frac{1}{pC_{int}R_{int}}. \tag{2.6}$$

We can consider (2.6) in a matrix form:

$$\mathbf{v}(p) = \frac{1}{pC_{int}R_{int}}\left(p\mathbf{I} + \frac{\eta}{C_{int}R_{int}}\mathbf{E}^{-1}\Lambda\mathbf{E}\right)^{-1}\mathbf{A}^{-1}\mathbf{b}, \tag{2.7}$$

where $\mathbf{E}$ is the transform matrix and Λ is the matrix of eigenvalues, $\mathbf{I}$ is a unity matrix, and the rest of symbols is of unchanged meaning. According to [10], we can define new variables $\mathbf{v}' = \mathbf{E}^{-1}\mathbf{v}$, $\mathbf{b}' = \mathbf{E}^{-1}\mathbf{b}$ and rewrite (2.7) to

$$\mathbf{v}' = \frac{1}{pC_{int}R_{int}}\left(p\mathbf{I} + \frac{\eta}{C_{int}R_{int}}\Lambda\right)^{-1}\mathbf{A}^{-1}\mathbf{b}'. \tag{2.8}$$

Then, we yield

$$T_j = \frac{R_{int}C_{int}}{\eta\lambda_j}, \tag{2.9}$$

where T_j represents time constants of uncoupled modes [10]. The time constant can be seen to be influenced by the learning constant η, which is represented by the value of R_f, by the integration constant $R_{int}C_{int}$ and by eigenvalues λ of the matrix $\mathbf{W}$.

This causes many problems in real-time applications: if ratio of eigenvalues is too high, time constants of uncoupled modes are very different, which results in long convergence time (computer simulations show, that for the eigenvalue ratio of two-dimensional Wang network $\lambda_2/\lambda_1=7$, the optimal convergence time is 41.44 μs, and for $\lambda_2/\lambda_1=70000$, the optimal convergence time is 20.52 ms). Moreover, if optimal setting of ANN parameters for the ratio $\lambda_2/\lambda_1=7$ is used, an undesired state of ANN is obtained when changing ratio to $\lambda_2/\lambda_1=70000$. In order to avoid this, parameters of ANN should be designed for $\lambda_2/\lambda_1=70000$, which causes long convergence time. Therefore, some improvements of the Wang network were developed in order to decrease the dependency of the convergence rate upon the eigenvalue ratio.

Trying to obtain as high convergence rate as possible, instability can be excited if real opamps are considered as shown in the next section. Therefore, the goal is to find the stable state with the maximal convergence rate.

2.1.1 Analysis of Wang ANN containing a real opamp

The instability of the real Wang ANN is caused by high gain of its closed loops as shown later. If the 2-dimensional network with real opamps is assumed, then three types of closed loops can be found in the system: the first one is inside the model of a real opamp (recursive definition of I_3 – see bellow), the second one is a feedback of the opamp (see Fig. 2.1), representing a mathematical operation in the circuit (integration, e.g.), and the third one is the feedback of the neuron as depicted in Fig. 2.1. The gain of the last closed loop is influenced by elements of the matrix **W** (represented by resistors $R_{i,j}$) and by the adaptive parameters of the network (time constants $R_{int}C_{int}$ and the learning constant η), the gain of the feedback of opamp is influenced by the learning constant η. Therefore, all the mentioned parameters can influence stability of the system. Further, we will discuss this influence.
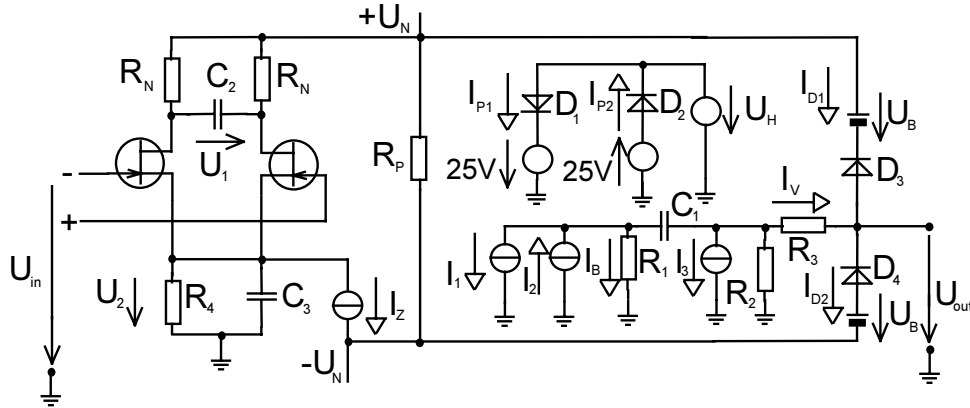

Fig. 2.2: Model of a real operational amplifier

The considered opamp model can be described by the following equations [4]:

$$I_1 = AU_1, \qquad\qquad (2.10)$$
$$I_2 = BU_2, \qquad\qquad (2.11)$$
$$U_H = HI_V, \qquad\qquad (2.12)$$

$$I_3 = CI_B + DI_{P1} - DI_{P2} - EI_{D1} + EI_{D2}, \tag{2.13}$$

where A to H are constants (see [4]) and the rest of symbols can be seen in Fig. 2.2.

The exact analysis of the multi-dimensional Wang ANN containing models of real opamps is rather difficult because of very complicated mathematical description. But, such analysis is not needed, because we can analyze one-dimensional Wang ANN and extend results to N dimensions. Nevertheless even in this case, some simplifications have to be done due to presence of non-linear circuit elements (diodes D_1 to D_4), e.g. Moreover, because of big complexity of the real opamp model, this model is considered being in the summing amplifier only. In the integrating amplifier and the inverting one, the ideal opamps are considered.
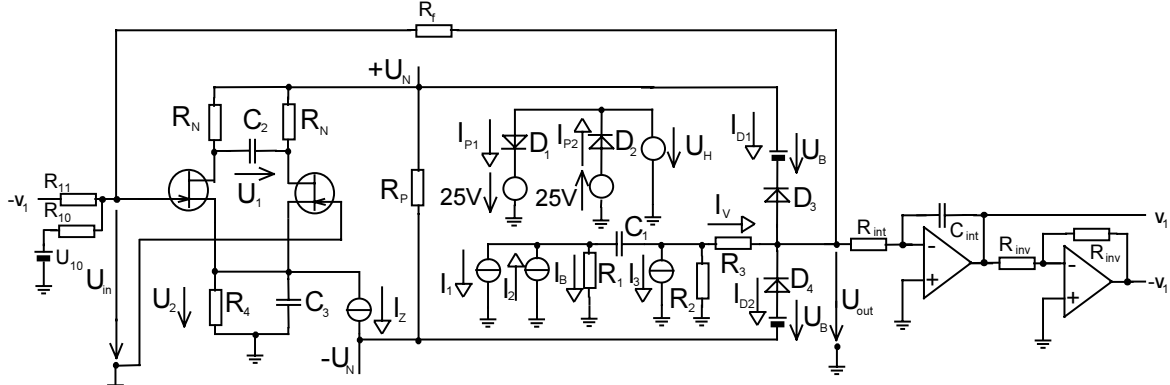

Fig. 2.3: Non-simplified version of the analyzed circuit

In the analyzed circuit, there are two feedbacks from the point of view of voltages on the input of the opamp U_{in} and on its output U_{out}. The first feedback is represented by the connection of input and output of the opamp through feedback resistor R_f in the summing amplifier, and the second one by the connection through resistor R_{11} (see Fig. 2.3). On the presence of these feedbacks, our analysis is based.

In the first step, the first feedback is handled. For this purpose, some simplifications are done. Computer simulations show, that the input part of the circuit (the differential amplifier in the opamp) can be described in a rather simple way because both the capacitor C_3 and the current source I_Z can be neglected (they do not significantly influence dynamics and stability of the network). JFETs can be assumed to work in the linear regime (small signals are expected).

Further, the non-linear sub-circuit in Fig. 2.3 can be neglected in order to simplify the analysis. After this simplification, the output voltage $U_{out}(p)$ can be expressed as

$$U_{out}(p) = \frac{C_{int}U_{10}R_{int}R_{11}R_a(\alpha p^3 + \beta p^2 + \gamma p + \xi)}{C_{int}p^4 + (C_{int}\delta + \varepsilon)p^3 + (C_{int}\varphi + \sigma)p^2 + (C_{int}\phi + \chi)p + \psi}, \tag{2.14}$$

where Greek symbols represent relatively complicated expressions containing the circuit parameters of the circuit from Fig. 2.3 (because of high number of complicated expressions, these relations are not presented here; detailed information about this analysis can be found in thesis). Since the polynomial in the denominator of $U_{out}(p)$ is of fourth order, the poles cannot be practically computed by the classical analytical means (numerical methods have to be used). The time course of

the error signal described by (2.14) has in the case of inappropriate setting of adaptive parameters the form of sinusoidal divergent signal described by relation

$$U_{out} = \frac{X_1 p + X_2}{p^2 + \omega_1^2} - \frac{X_3 p + X_4}{(p+b)^2 + \omega_2^2} . \qquad (2.15)$$

This expression in time domain represents the difference between fixed oscillations and depressed ones, which corresponds with rising oscillations that become stable after certain time. This time is given by a parameter b in (2.15).

From comparison of (2.15) and (2.14), we can get

$$b = \frac{C_{int}\delta + \varepsilon}{2C_{int}} , \qquad (2.16)$$

$$\omega_1^2 = \frac{C_{int}\phi + \chi}{C_{int}\delta + \varepsilon} , \qquad (2.17)$$

$$\omega_2^2 = \left(\frac{2\psi}{C_{int}\phi + \chi} - \frac{C_{int}\delta + \varepsilon}{2C_{int}} \right) \frac{C_{int}\delta + \varepsilon}{2C_{int}} . \qquad (2.18)$$

Relations (2.16) to (2.18) show, that existence of this state depends on many ANN parameters and properties of the input signal matrix. For the use of the real Wang ANN, it is important to find the condition for transition from the stable state (which is described by (2.14) with polynomial in denominator with negative nonzero real parts of all poles) to the state described by (2.15), but these conditions are practically not possible to find by analytical means. Dependence of the error signal on the ratio of eigenvalues of input signal matrix can be obtained by using the above-described matrix transform - we replace R_{11} by the matrix $R_f(\eta \mathbf{A}^T \mathbf{A})^{-1}$ and turn it to $(\eta \mathbf{E}^{-1} \Lambda \mathbf{E})^{-1}$, as was mentioned above. Nevertheless, the dependence of $U_{out}(p)$ on ratio of eigenvalues is rather complicated and difficult to discuss, because the resistor R_{11} occurs in many serial and parallel combinations of resistors, which were replaced by many symbols simplifying presented relations as R_a, R_{ax} etc. (for details, see thesis), therefore it will be not discussed here. We can conclude that the performed analysis resulted in the exact description of the "real" Wang ANN behavior, which is much more complicated in comparison with [13] and which shows the ANN stability depending on many parameters of the used opamp model, on parameters of the network and on parameters of the input signal matrix. Of course, we can consider that most of them need not be changed during use of the network, but we must always consider changes of eigenvalues of the input signal matrix. Because these changes can cause unpleasant consequences, we must think about elimination of such influences. Possibilities of the solution of this problem are discussed bellow.

2.1.2   Exploitation of Compton loop in Wang ANN

Recently, principle of Compton version of an analog control algorithm [9] is used in digital neural networks in order to improve their properties. The following relation can describe the circuit from Fig. 2.4:

$$v_1(p) = R_f \left[\frac{U_1}{pR_1} - \frac{v_1(p)}{R_{11}} - \frac{v_1(p)pC_{int}R_{int}}{R_{11}} \right] \frac{1}{pC_{int}R_{int}}. \qquad (2.19)$$

Using similar matrix transform, we can obtain

$$\mathbf{v}'(p) = \frac{1}{p} \left[pC_{int}R_{int}(\mathbf{I} + \eta\Lambda) + \eta\Lambda \right]^{-1} \mathbf{A}^T \mathbf{b}'. \qquad (2.20)$$

The time constants of uncoupled modes of $\mathbf{v}(t)$ can be expressed as

$$T_j' = \frac{R_{int}C_{int}(1 + \eta\lambda_j)}{\eta\lambda_j} = R_{int}C_{int}\left(1 + \frac{1}{\eta\lambda_j}\right), \qquad (2.21)$$

where λ_j is j-th eigenvalue of the matrix product $\mathbf{A}^T\mathbf{A}$. Comparing relations (2.20) and (2.21) with relations describing classical Wang ANN, we can see weaker dependence of convergence rate on the eigenvalue ratio. Nevertheless, the convergence rate is still dependent on the time constant of the integrator.

Comparison of relations describing the Compton version of the Wang ANN and classical Wang ANN shows that Compton version of Wang ANN converges more slowly than the classical Wang ANN. On the contrary, computer simulations demonstrate that the Compton version converges more quickly for all observed eigenvalue ratios of the matrix $\mathbf{W}$. For $\lambda_2/\lambda_1=70000$, the convergence time of the Compton version is 150.0 µs compared to 20.52 ms for the classical one. For $\lambda_2/\lambda_1=700$, the convergence time of the Compton version is 79.03 µs compared to 385.61 µs for the classical one and for $\lambda_2/\lambda_1=7$, the convergence time of the Compton version is 3.42 µs compared to 41.44 µs for the classical one. The difference between theoretical conclusions and results of computer simulations can be explained by neglecting real circuit properties in the above-presented derivations.
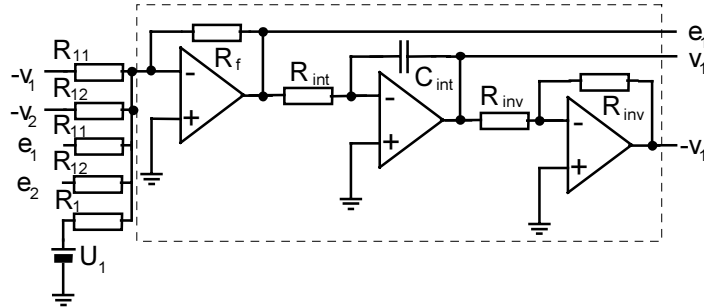

Fig. 2.4: Compton version of the first neuron of the one-dimensional Wang ANN

2.1.3 Modification of Wang ANN toward better convergence rate

Since convergence properties of Wang ANN are rather poor, we turned our attention to their improvement. This goal can be reached by several ways.

The use of a non-linear element in Wang ANN

In order to improve the convergence, we have to consider the above-mentioned negative properties of used opamps, which cause limiting of the convergence rate.

For ideal Wang ANN, time constant is given by

$$T = \frac{R_{int} C_{int} R_{11}}{R_f}.$$ (2.22)

Hence, the minimal convergence time equals to zero - if the time constant $R_{int} C_{int}$ approaches zero, we can find from the relation describing time course of solution

$$v_1(t) = \frac{U_1 R_{11}}{R_1} \left[1 - \exp(-t/T)\right],$$ (2.23)

that the convergence time approaches zero.

The bellow-limited convergence time of Wang ANN is caused by a potential unstable state, appearing when the gain of one of closed loops is too high. Consequently, only a certain minimal nonzero convergence time depending on circuit parameters, which influence the gain of closed loops, can be reached.

Generally, it is possible to afford higher gains of closed loops in the beginning of convergence process compared to the gains corresponding to the mentioned minimal convergence time, when the circuit parameters are independent on time. This leads to the increase of the convergence rate, which can be realized through a non-linear time constant with small starting value, which is increased with time. This idea can be realized by replacing of the resistor R_{int} by two contra-parallel diodes (Fig. 2.5). The parallel resistor R_p ensures a minimal convergence rate when the voltage over diodes is smaller then their threshold voltage, the serial resistor R_s limits the resistance between output of the summing amplifier and input of the integrator (a certain minimal value of this resistance ensures a stable state of the network).

In the analysis, we consider one-dimensional Wang ANN and an ideal diode (described according to [5]). Because of simplicity of the analysis, the resistors R_p and R_{si} are neglected. That way, we obtain the error signal

$$e_1(t) = U_T \ln\left[\frac{e^{\beta}\left(1 + e^{-\alpha}\right) + 1 - e^{-\alpha}}{e^{\beta}\left(1 - e^{-\alpha}\right) + 1 + e^{-\alpha}}\right],$$ (2.24)

where

$$\alpha = \frac{2 R_f I_0}{C_{int} R_{11} U_T} t,$$ (2.25)

$$\beta = -\frac{U_1 R_f}{U_T R_1}$$ (2.26)

and

$$U_T = kT/q.$$ (2.27)

In (2.27), k is a Boltzman constant, q is a charge of electron, and T is temperature in Kelvin scale. Replacing the left side of (2.24) by ε, we obtain the convergence time when error signal reaches the value ε as

$$t_\varepsilon = \frac{U_T R_{11} C_{int}}{2 I_0 R_f} \ln\left[\frac{1 + \exp(-\varepsilon/U_T)}{1 - \exp(-\varepsilon/U_T)} \frac{1 - \exp(-\beta)}{1 + \exp(-\beta)} \right]. \qquad (\,2.28\,)$$

Considering $e_1(0) \gg U_T$ and $\varepsilon = U_T$, the argument of the logarithm in (2.28) goes to one. Under the conditions that $R_{int} = U_T/2 I_0$ and other circuit parameters are in both networks the same, the convergence time for certain ε and $e_1(0)$ is shorter for the modified Wang ANN. The reason is, that the conductance of diodes in the modified Wang ANN is very low at the beginning of the convergence process and during this process rises with time. The convergence time can be shortened by the use of the resistor R_p (see Fig. 2.5), because the conductance of diodes for error signal close to zero approaches infinity, which significantly decreases the convergence rate, and this parallel resistor then ensures a certain minimal convergence rate. Unfortunately, we cannot compute a relation for the time course in this case.
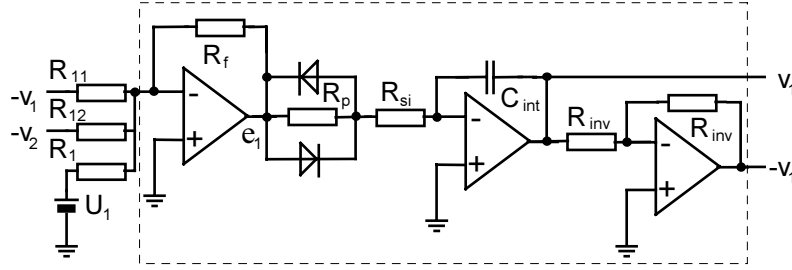

Fig. 2.5: First neuron of Wang ANN with non-linear time constant

The above-presented theoretical conclusion is confirmed by results of computer simulations. For $\lambda_2/\lambda_1 = 70000$, the convergence time of the modified ANN equals to 64.29 µs versus 20.52 ms of the classical one. For $\lambda_2/\lambda_1 = 700$, the convergence time of the modified ANN equals to 69.64 µs versus 385.61 µs of the classical one and for $\lambda_2/\lambda_1 = 7$, the convergence time of the modified ANN equals to 2.75 µs versus 41.44 µs of the classical one.

Parallel combination of the integration resistor and a capacitor in Wang ANN

The integrating resistor is substituted by the parallel combination of a resistor and a capacitor in this modification. The analysis of such circuit requires considering instead of an ideal opamp an inverting amplifier with a gain described at least by

$$G(p) = \frac{-G}{1 + p\tau}. \qquad (\,2.29\,)$$

Here, G and τ are constants. The voltage $v_1(p)$ can be expressed (considering instead a block with $G(p)$ an ideal opamp and a resistor R_3 as being zero) as

$$v_1(t) = \frac{U_1 R_{11}}{R_1} - \left[\frac{U_1 R_{11}}{R_1} - \frac{U_1 R_f C_d R_{11}}{(C_{int} R_{11} + R_f C_d) R_1} \right] \exp\left[\frac{-R_f t}{(C_{int} R_{11} + R_f C_d) R_{int}} \right]. \qquad (\,2.30\,)$$

Now, we can compare the time constant of the analysed circuit

$$T_a = \left(C_{int} R_{11} + R_f C_d \right) R_{int} / R_f \qquad (2.31)$$

with the relation for the time constant of the classical Wang ANN

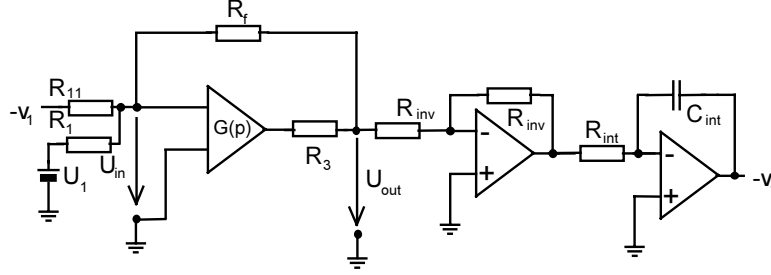$$T_c = R_{int} C_{int} R_{11} / R_f . \qquad (2.32)$$

Fig. 2.6: The analysed circuit

Comparing (2.31) and (2.32), the time constant of the novel ANN is always higher than the time constant of the classical Wang ANN, i.e. the novel ANN should converge more slowly. On the other hand, if the gain of the summing amplifier is given by (2.29), the time constants of the novel ANN can be smaller (under certain conditions) than in the classical Wang ANN with the same summing amplifier.

First, the classical Wang ANN from Fig. 2.6 is discussed. We consider the opamp having the gain described by (2.29) instead of an ideal opamp in the summing amplifier (the other opamps we consider as ideal). First, we consider an amplifier to be given by the gain -*G* only. Then, the time course of U_{out} can be described as

$$U_{out}(t) = \frac{U_1 X_1 (X_2 - GX_3)}{X_4 (X_5 + GR_f R_a)} \, \exp\!\left(-\frac{t}{T} \right), \qquad (2.33)$$

where

$$X_1 = R_{11} C_{int} R_{int} R_f , \qquad (2.34)$$

$$X_2 = R_3 (R_3 + R_f)(R_f + R_a) + R_3^2 R_f , \qquad (2.35)$$

$$X_3 = (R_f + R_a)\left[R_f (R_3 + R_f) + R_3 R_f \right] - R_3 R_f R_a , \qquad (2.36)$$

$$X_4 = C_{int} R_{int} (R_{11} + R_1)\left[(R_3 + R_f)(R_f + R_a) + R_3 R_f \right], \qquad (2.37)$$

$$X_5 = (R_3 + R_f)(R_f + R_a) + R_3 R_f , \qquad (2.38)$$

and

$$T = \frac{X_4 (X_5 + GR_f R_a)}{R_1 R_f \left[GX_6 - R_3 (X_5 + GR_f R_a) \right]} . \qquad (2.39)$$

Now, we consider that the amplifier with the gain $G(p)$ in the non-ideal summing amplifier is described by (2.29). Then, poles of U_{out} are of the form

$$p_{1,2} = \frac{-b \pm \sqrt{b^2 - 4X_4 X_5 \tau (GX_6 - R_3 GR_f R_a - R_3 X_5) R_1 R_f}}{2X_4 X_5 \tau}, \qquad (2.40)$$

where

$$b = X_4 X_5 + GR_f R_a X_4 - R_1 R_f R_3 X_5 \tau \qquad (2.41)$$

and

18

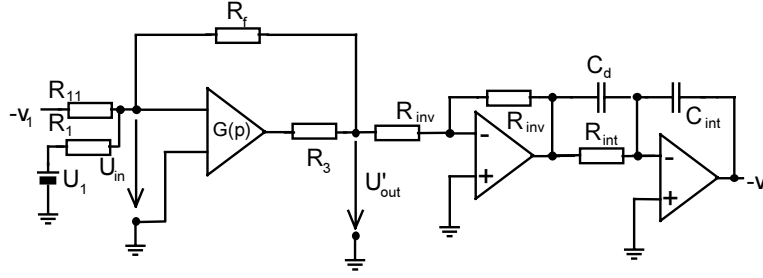$$X_6 = (R_f + R_a)\left[R_f(R_3 + R_f) + R_3 R_f\right]. \qquad (2.42)$$

Fig. 2.7: Improvement of the convergence rate of Wang ANN

Considering the novel Wang ANN (Fig.2.7) and assuming the gain $G(p)$ of the amplifier given by (2.29), the poles of U'_{out} can be expressed as

$$p_{1,2} = \frac{-b' \pm \sqrt{b'^2 - 4X_5\tau(X_4 - R_1 R_f R_3 R_{int} C_d)X_7}}{2X_5\tau(X_4 - R_1 R_f R_3 R_{int} C_d)}, \qquad (2.43)$$

where

$$b' = X_4(X_5 + GR_f R_a) - R_1 R_f R_3 X_5 \tau + X_7 R_{int} C_d \qquad (2.44)$$

and

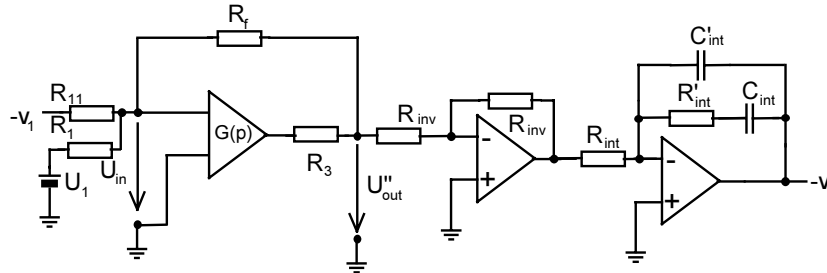$$X_7 = R_1 R_f\left[GX_6 - R_3(X_5 + GR_f R_a)\right]. \qquad (2.45)$$

Fig. 2.8: Another improvement of the convergence rate of Wang ANN

Comparing (2.43) and (2.40), we can conclude that under condition of certain circuit-parameters setting (of course, corresponding circuit parameters have in both networks the same values), convergence time of the modified circuit is shorter, which is in opposite to the comparison of time courses of ideal circuits.

This conclusion is confirmed by results of computer simulations. For λ_2/λ_1=70000, the convergence time of the novel ANN is 377.01 µs versus 20.52 ms of the classical Wang ANN. For λ_2/λ_1=700, the convergence time of the novel ANN is 131.88 µs versus 385.61 µs of the classical Wang ANN and for λ_2/λ_1=7, the convergence time of the novel ANN is 31.89 µs versus 41.44 µs of the classical one.

Serial combination of the integration capacitor and a resistor in Wang ANN

The modification is depicted in Fig. 2.8. Here, we consider a constant-gain amplifier only in order to obtain simpler description. Then, it can be obtained

$$U''_{out}(p) = \frac{U_1 R_{11} R_{int} R_f (X_2 - GX_3)(C_{int} + C'_{int} + pC'_{int}C_{int}R'_{int})}{pX_9(C_{int} + C'_{int} + pC'_{int}C_{int}R'_{int})(X_5 + GR_f R_a) - X_8(pC_{int}R'_{int} + 1)}, \quad (2.46)$$

with

$$X_8 = R_1 R_f \left[R_3(X_5 + GR_f R_a) - GX_6 \right], \quad (2.47)$$

$$X_9 = R_{int}(R_{11} + R_1)\left[(R_3 + R_f)(R_f + R_a) + R_3 R_f \right], \quad (2.48)$$

C'_{int} and R'_{int} are depicted in Fig. 2.8 and the rest of symbols was already explained. This relation can be rewritten to

$$U''_{out}(p) = \frac{pU_1 R_{11} R_{int} R_f (X_2 - GX_3)C'_{int}C_{int}R'_{int}}{p^2 \left[C_{int}C'_{int}R'_{int}X_9(X_5 + GR_f R_a) \right] + p\beta - X_8} +$$

$$+ \frac{U_1 R_{11} R_{int} R_f (X_2 - GX_3)(C_{int} + C'_{int})}{p^2 \left[C_{int}C'_{int}R'_{int}X_9(X_5 + GR_f R_a) \right] + p\beta - X_8}, \quad (2.49)$$

where

$$\beta = (C_{int} + C'_{int})X_9(X_5 + GR_f R_a) - C_{int}R'_{int}X_8, \quad (2.50)$$

and the poles of (2.46) can be expressed as

$$p_{1,2} = \frac{-\beta \pm \sqrt{\beta^2 - 4C_{int}C'_{int}R'_{int}X_9(X_5 + GR_f R_a)R_1 R_f \left[GX_6 - R_3(X_5 + GR_f R_a) \right]}}{2C_{int}C'_{int}R'_{int}X_9(X_5 + GR_f R_a)}. \quad (2.51)$$

Comparing (2.51) and (2.33), the voltage $U''_{out}(p)$ can be found to converge more quickly to zero (under condition of certain setting of circuit parameters - of course, the corresponding circuit parameters have in both networks the same values), which is again in opposite to the comparison of ideal circuits.

This conclusion is confirmed by results of computer simulations. For $\lambda_2/\lambda_1 = 70000$, the convergence time of the modified ANN (Fig. 2.8, SRIC-ANN, instead of the block with $G(p)$ is used a real opamp and the value of R_3 is set to zero) is 93.75 µs versus 20.52 ms of the classical Wang ANN. For $\lambda_2/\lambda_1 = 700$, the convergence time of SRIC-ANN is 45.54 µs versus 385.61 µs of the classical Wang ANN and for $\lambda_2/\lambda_1 = 7$, the convergence time of SRIC-ANN is 2.05 µs versus 41.44 µs of the classical Wang ANN.

2.2 ANN BASED ON SIMPLIFIED KALMAN FILTER

In this section, the recurrent analog neural network (ANN) based on the simplified Kalman filter (SKF) is analyzed. On the basis of analysis results, improvements of the simplified Kalman network (SKN) are proposed.

2.2.1 Description of Kalman filter based ANN

Application of Kalman filter theory to Wang ANN [7] removes negative features of Wang ANN (low convergence rate, e.g.). Applying Kalman filter to the solution of the simultaneous set of linear equations, following relations are obtained [7]:

$$\frac{d\mathbf{v}(t)}{dt} = \mathbf{K}(t) \cdot [\mathbf{b} - \mathbf{A} \cdot \mathbf{v}(t)], \qquad (2.52)$$

$$\mathbf{K}(t) = \mathbf{P}(t) \cdot \mathbf{A}^{\mathrm{T}} \cdot \mathbf{R}^{-1}, \qquad (2.53)$$

$$\frac{d\mathbf{P}(t)}{dt} = -\mathbf{K}(t) \cdot \mathbf{A} \cdot \mathbf{P}(t). \qquad (2.54)$$

Here, $\mathbf{P}(t)$ is a predicted state-error, $\mathbf{R}^{-1}$ is inverted correlation matrix of a residual error, $\mathbf{K}$ denotes a matrix of a Kalman gain, $\mathbf{A}$ is the matrix of coefficients of solved set of equations, $\mathbf{b}$ denotes the column vector of right-hand sides of solved equations, and $\mathbf{v}$ is the column vector of solution.
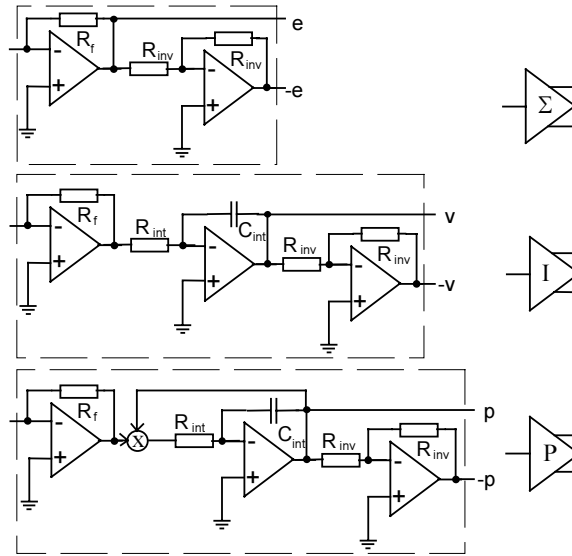

Fig. 2.9: Neurons used in the Kalman ANN:
a) summing amplifier, b) integrator, c) predictor

Pure Kalman filter is very complicated, and therefore, its simplified version was developed [7]. Simplification consists in use of diagonal elements of matrix $\mathbf{P}(t)$ only.

In analog realization, simplification decreases the number of circuit elements (analog multipliers, especially). Therefore, the simplified version of Kalman filter (SKF) is used as a basis of ANN developed in this chapter. Discussion of convergence properties of SKF was published in [6]: the paper concludes that convergence properties of SKF approach pure Kalman filter on one hand and LMS algorithm on the other hand. Unfortunately, mathematical description of SKF is rather complicated. Therefore, we will use in following the mathematical description of the pure Kalman filter (eqns. 2.52 to 2.54) only, which leads to the same result if only one-dimensional network is considered (which is discussed first).

SKN is depicted in Fig. 2.10. The difference between the pure Kalman ANN and SKN is hidden in the upper sub-circuit, which is very complicated for the pure Kalman ANN (and therefore, it is not depicted here). All the modifications, which are presented in this chapter, are therefore based on SKF.
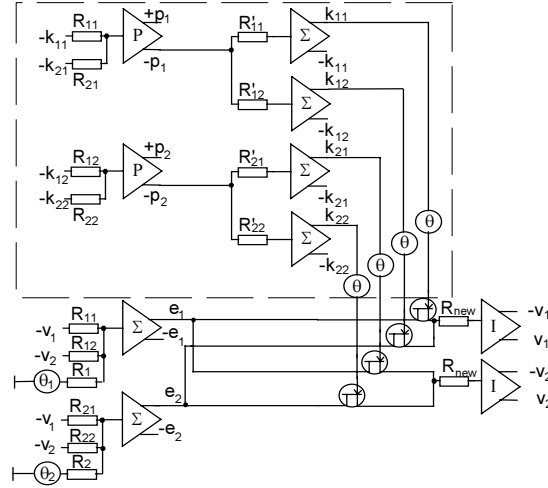
Fig. 2.10: Analog realization of SKN for solving set of simultaneous linear equations

SKN consists of three types of neurons (Fig. 2.9): of a summing amplifier, an integrator and a predictor (it computes diagonal elements of the predicted state-error correlation matrix). In the predictor, a circle containing $\times$ denotes an analog multiplier. The Kalman gain is led to integrators by JFETs, which serve as electrically controlled resistors. Bias points of JFETs are set by DC sources θ_m. Elements of the matrix $\mathbf{A}$ are interpreted in the circuitry by resistors $R_{m,n}$, $R'_{m,n}$

$$R_{m,n} = R_f / \eta a_{m,n}, \qquad (2.55)$$

$$R'_{m,n} = R_f / \rho a_{m,n}, \qquad (2.56)$$

where R_f is a feedback resistor of an input opamp of the respective neurons, $a_{m,n}$ is an element of the matrix $\mathbf{A}$, η is an adaptation constant and

$$\rho = R^{-1} > 0. \qquad (2.57)$$

If $R < 0$ ($R > 0$), the respective negative (positive) neuron output is used. If $a_{m,n} < 0$, then the negative output of the $k_{m,n}$ neuron is led to the gate of the JFET and the negative output of the e_m neuron is led to its drain. Inverted output ($-k_{m,n}$) is connected to the input of the predictor through the resistor $R_{m,n}$ (see Fig. 2.10) and positive output of the integrator is connected to the respective resistor $R_{m,n}$. Resistors and sources of the biasing thresholds of neurons are associated by

$$b_m = \frac{\theta_m R_f}{\eta R_m}, \qquad (2.58)$$

where b is an element of the vector $\mathbf{b}$ and R_m is the resistance between the voltage source and the summing amplifier. JFETs in Fig. 2.10 are serving as controlled resistors, θ is a threshold for a JFET, and a resistor R_{new} ensures stability of the circuit in the case when the resistance of a JFET is small.

2.2.2   Analysis of SKN

For simplicity of the outcome of the analysis, only ideal one-dimensional SKN is discussed first. The analysis of SKN is quite complicated, and therefore, some

simplifications have to be done. Feedback resistors in summing amplifiers and time constants are considered to be the same in the whole circuitry. Next, JFET (plus R_{new}) and following summing amplifier in the integrator are represented by the product of Kalman gain and error signal. The solution $v(t)$ can be expressed as

$$v(t) = \frac{\theta_1 R_{11}}{R_1} \left[1 - \frac{R_{11} R_{11}' C_{int} R_{int}}{U_0 R_f^2 t + R_{11} R_{11}' C_{int} R_{int}} \right]. \qquad (2.59)$$

The vector of solutions can be expressed by rewriting of (2.59) to matrix form:

$$\mathbf{v}(t) = \left[\mathbf{I} - \left(\mathbf{A}\, \mathbf{A}^\mathrm{T}\, \frac{U_0 \eta \rho t}{C_{int} R_{int}} + \mathbf{I} \right)^{-1} \right] \mathbf{A}^{-1}\, \mathbf{b}. \qquad (2.60)$$

We can use the above-described matrix transform in order to obtain the dependence on eigenvalues: we can define new variables $\mathbf{v'} = \mathbf{E}^{-1}\, \mathbf{v}$, $\mathbf{b'} = \mathbf{E}^{-1}\, \mathbf{b}$, where $\mathbf{E}$ denotes a transform matrix. We multiply (2.60) by $\mathbf{E}^{-1}$ and rewrite it to

$$\mathbf{v'}(t) = \left[\mathbf{I} - \left(\Lambda \frac{U_0 \eta \rho t}{C_{int} R_{int}} + \mathbf{I} \right)^{-1} \right] \mathbf{A}^{-1}\, \mathbf{b'} = \left[\mathbf{I} + \frac{C_{int} R_{int}}{U_0 \eta \rho t} \Lambda^{-1} \right]^{-1} \mathbf{A}^{-1}\, \mathbf{b'}. \qquad (2.61)$$

Here, Λ represents the matrix of eigenvalues. Comparing Wang ANN and SKN, the form of the convergence process of Wang ANN is given by the exponential function of a negative argument. If the argument is a function of time, decrease of such exponential function is quicker than decrease of the inverted value of time. But, computer simulations show that SKN converges more quickly for the same input signal, which can be explained by the influence of real circuit elements (see above). Higher convergence rate of SKN is caused by multiplying the error signal by the Kalman gain, which is decreasing with time very quickly. Therefore, the gains of the closed loops in the lower part of SKN are not time-independent - they are decreasing in time due to described multiplying. Hence, creating an unstable state requires higher values of gains of closed loops at the beginning of the convergence process comparing to Wang ANN, which leads to better convergence. It must be also noted, that the Kalman gain depends also on the upper-circuit adaptation parameters, which allows finer tuning of the network.

The results of computer simulations show that convergence time for all the observed eigenvalue ratios is significantly shorter at SKN comparing to the classical Wang ANN. For $\lambda_1/\lambda_2 = 7$, the optimal convergence time of SKN is 2.19 μs versus 41.44 μs of Wang ANN. For $\lambda_1/\lambda_2 = 700$, the optimal convergence time of SKN is 101.46 μs versus 385.61 μs of Wang ANN, and for $\lambda_1/\lambda_2 = 70000$, the optimal convergence time of SKN is 789.27 μs versus 20.52 ms of Wang ANN. On the other hand, the above-presented improvements of Wang ANN exhibit better (or approximately the same) convergence rate than SKN.

The essential drawback of SKN is the stability dependence on the eigenvalue ratio. If optimally set circuit parameters are used for another eigenvalue ratio, SKN starts to diverge (except of the case $\lambda_1/\lambda_2 = 7$, when circuit parameters are optimally

set for λ_1/λ_2=70000). Moreover, for λ_1/λ_2=70000, SKN converges for upper-part parameter setting in a relatively narrow neighborhood of theirs optimal values only.

Considering the above-given discussion, SKN is not appropriate for the real-time processing. Further, confrontation of SKN and improved Wang ANN shows similar convergence properties of networks on one hand and more complicated circuitry of SKN on the other hand. Therefore, improvements of SKN have to be proposed.

2.2.3 Improved versions of SKN

All the improvements we have developed for Wang ANN were applied even to SKN. Since both the principles and the analysis methods are similar, we concentrate to the discussion of the results here.

SKN with additional feedback

In the lower sub-circuit, two possible feedbacks can be created following the idea of Compton loop. The feedback can connect the output of summing amplifier and its input (as done at Wang ANN), or can connect the input of integrator and the input of summing amplifier (see Fig. 2.11). The second solution provides better properties of SKN due to involving Kalman-gain multiplication in the closed loop. The analysis of this network leads to relation

$$v(t) = \frac{\theta_1 R_{11} R_f^2 U_0 t}{R_1 \left[R_f^2 t U_0 + C_{int} R_{int} (R_{11} R'_{11} + R_f^2 U_0) \right]}. \qquad (2.62)$$

Exploiting the above mentioned transform, eqn. (2.62) can be expressed as

$$\mathbf{v}'(t) = \left\{ \mathbf{I} + \frac{R_{int} C_{int}}{t} \Lambda^{-1} \left[\Lambda + \frac{1}{\eta \rho U_0} \right] \right\}^{-1} \mathbf{A}^{-1} \mathbf{b}'. \qquad (2.63)$$

Comparing classical SKN and improved one, weaker dependency of convergence rate on eigenvalue ratio can be seen. In (2.61), time is multiplied by $\Lambda \eta U_0 \rho / C_{int} R_{int}$ versus $\Lambda \{ [\Lambda + (\eta \rho U_0)^{-1}] C_{int} R_{int} \}^{-1}$ in (2.63). Improved convergence properties are illustrated by results of computer simulations: convergence time for all the examined eigenvalue ratios is much better comparing to classical SKN. For λ_1/λ_2=7, the optimal convergence time of improved SKN is 587 ns versus to 2.19 μs of the classic one. For λ_1/λ_2=700, the optimal convergence time of the improved SKN is 3.22 μs versus to 101.46 μs of the classic one. For λ_1/λ_2=70000, the optimal convergence time of the improved SKN is 23.30 μs versus 789.29 μs of the classical one. If the optimal setting of circuit parameters for λ_1/λ_2=7 and λ_1/λ_2=700 is used in the case of λ_1/λ_2=70000, AF-SKN diverges. On the other hand, AF-SKN with optimal setting for λ_1/λ_2=70000 converges even for eigenvalue ratio 7 and 700. In the first case, the convergence time is 17.33 μs, in the second one 161.43 μs.
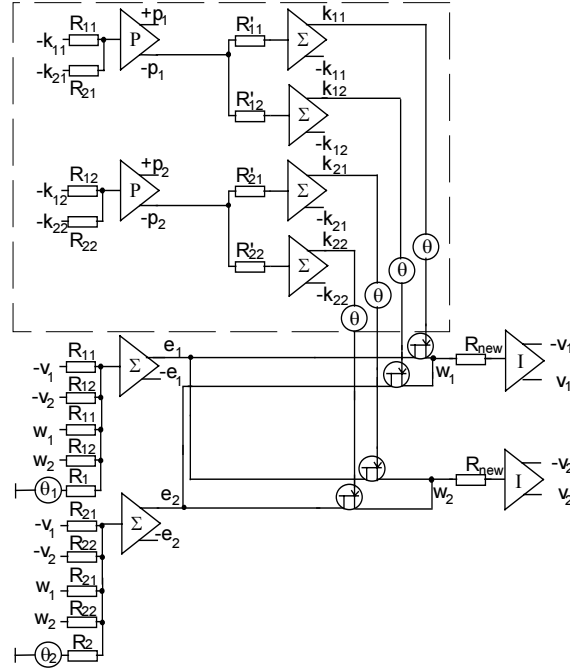
Fig. 2.11: Analog realization of SKN with an additional feedback

We can conclude, that AF-SKN significantly improves convergence properties of SKN. On the other hand, AF-SKN still exhibits relatively high dependence of the convergence rate on the circuit parameters and on the eigenvalue ratio.

SKN with modified Kalman-gain course

A higher convergence rate can be reached by the low-pass filtering of the Kalman gain (see Fig. 2.12). Unfortunately, an analysis of such modified SKN leads to rather complicated expressions, which will be therefore not presented here. Computer simulations show that only the optimal convergence time of MKG-SKN for λ_1/λ_2=70000 is better (33.93 µs) comparing to classical SKN (789.29 µs). In other investigated cases, convergence time of MKG-SKN is longer comparing to classical SKN: for λ_1/λ_2=7, the optimal convergence time of MKG-SKN is 7.99 µs versus 2.19 µs of classical SKN, and for λ_1/λ_2=700, the optimal convergence time of MKG-SKN is 118.97 µs versus 101.46 µs of classical SKN.

The dependence of the convergence rate on the circuit parameters of MKG-SKN is a bit worse comparing to classical SKN. On the contrary, the dependence on circuit elements C_F and R_F is relatively low – wide-range variation of C_F and R_F causes neither divergence nor the significant change of the convergence time. MKG-SKN is advantageous in relatively short optimal convergence time for λ_1/λ_2=70000: for applying ANN, setting of circuit parameters for the highest used eigenvalue is needed in order to minimize risk of the unstable states. Therefore, the fact, that the optimal setting for λ_1/λ_2=70000 can be used for both the other investigated cases, is an advantage. For λ_1/λ_2=7, MKG-SKN converges in 16.58 µs, and for λ_1/λ_2=700, MKG-SKN converges in 1.35 ms. These results are worse than the results exhibited

by the circuit from Fig. 2.11, nevertheless, MKG-SKN is important as a part of the ANN from Fig. 2.14 (see bellow).
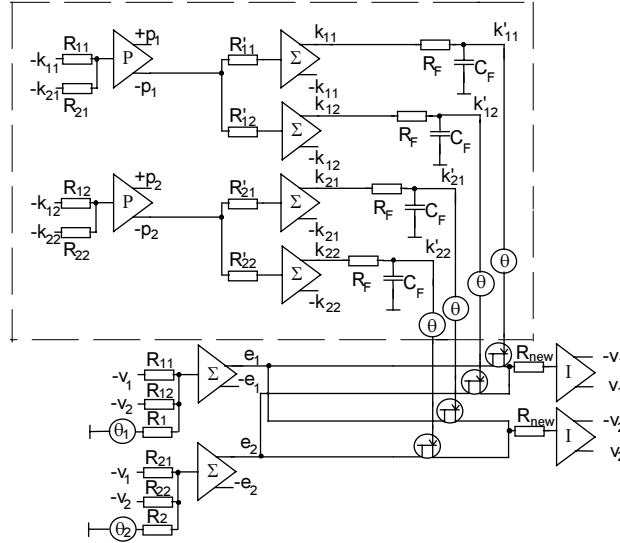

Fig. 2.12: Analog realization of SKN with modified predictor

SKN with modified integrator

This modification uses a resistor in series with C_{int} in integrator (see Fig. 2.13). The rest of the circuitry corresponds to the original circuitry, therefore, we have to derive the error signal and the solution only. The solution can be expressed as

$$v(t) = \frac{\theta_1 R_{11}}{R_1} \left[1 - \frac{\left(R_{int} C_{int} R_{11} R'_{11} + R_f^2 R'_{int} U_0 C_{int} \right)\left(U_0 R_f^2 t + R_{int} C_{int} R_{11} R'_{11} \right)}{\left(U_0 R_f^2 t + R_{int} C_{int} R_{11} R'_{11} + R_f^2 R'_{int} U_0 C_{int} \right)^2} \right]. \quad (2.64)$$

Eqn. (2.64) can be (using previously described transform) rewritten to

$$\mathbf{v}'(t) = \left[\mathbf{I} - \left\{ \left[\frac{t\Lambda}{C_{int} R_{int}} \left(\Lambda \frac{R'_{int}}{R_{int}} + \frac{1}{U_0 \eta \rho} \right)^{-1} + \mathbf{I} \right]\left[\frac{R'_{int}}{R_{int}} \left(\frac{t}{R_{int} C_{int}} + \frac{\Lambda^{-1}}{U_0 \eta \rho} \right)^{-1} + \mathbf{I} \right] \right\}^{-1} \right] \mathbf{A}^{-1}\mathbf{b}'. \quad (2.65)$$

The term in the first bracket equals to the expression in brackets in (2.63) if $R'_{int} = R_{int}$. In the second bracket, time is not multiplied by Λ, and therefore, there is small influence of this term to the convergence rate for t sufficiently high. Unfortunately, influence of this term occurs at the beginning of the convergence process, which cause some influence of the eigenvalue matrix because of multiplying by this term, which is disadvantage in comparison with (2.63).

Computer simulations show that only the optimal convergence time of the modified network for $\lambda_1/\lambda_2 = 70000$ is better comparing SKN in this case (83.93 μs versus 789.29 μs). In other investigated cases, modified ANN is worse: for $\lambda_1/\lambda_2 = 7$, the optimal convergence time of the modified ANN is 25.71 μs versus 2.19 μs of SKN, for $\lambda_1/\lambda_2 = 700$, the optimal convergence time of the modified ANN is 271.30 μs versus 101.46 μs of SKN.
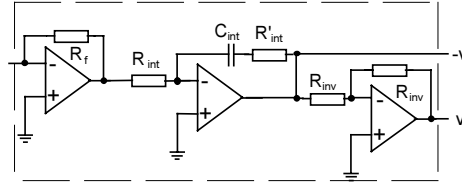
Fig. 2.13: Modified integrator

The dependence of the convergence rate on the circuit parameters is worse compared to SKN, because the network often converges only in a narrow neighborhood of the optimal value of the corresponding parameter. If the optimal setting of circuit parameters for $\lambda_1/\lambda_2=7$ and 700 is used for another eigenvalue ratio, then ANN diverges. If optimal setting is done for $\lambda_1/\lambda_2=70000$, then ANN converges for $\lambda_1/\lambda_2=7$ in 86.79 μs, and for $\lambda_1/\lambda_2=700$ in 346.25 μs. These results are slightly worse compared to Compton SKN, and better to MKG-SKN. The optimal convergence time (except of $\lambda_1/\lambda_2=70000$) is worse compared to the respective modification of Wang ANN. In the circuit depicted in Fig. 2.8, capacitor C'_{int} is used in contrast to modified SKN, which reduces some negative influences of the resistor R'_{int} to the convergence rate. Here, we discussed the circuit without this capacitor in order to reduce mathematical complexity. This modified SKN is important because of its relatively low dependence of the convergence rate on the eigenvalue ratio, and therefore, it is used in its improved version with capacitor C'_{int} (see Fig. 2.15) as one of main elements of the ANN from Fig. 2.14.

Combination of designed improvements

In order to obtain a very fast ANN of weak dependence of the convergence rate on eigenvalue ratio, several above-described improvements can be combined.

The results of computer simulations show, that such ANN is of the best convergence properties. For $\lambda_1/\lambda_2=7$, the combined SKN converges in 847.8 ns. For $\lambda_1/\lambda_2=700$, the combined SKN converges in 591.4 ns, and for $\lambda_1/\lambda_2=70000$, the convergence time is 1.21 μs. Further, the dependence of the convergence rate on the eigenvalue ratio is very low. If the optimal circuit-parameter setting for $\lambda_1/\lambda_2=70000$ is used, the combined SKN converges in 1.23 μs for $\lambda_1/\lambda_2=7$, and the convergence time for $\lambda_1/\lambda_2=700$ is 1.05 μs. I.e., the convergence time for all the examined eigenvalue ratios is practically the same. Next, computer simulations show that the convergence rate depends weakly on setting of the circuit parameters (much weaker compared the other SKN), except parameters R_F and C_F.

Unfortunately, time course of the combined SKN cannot be expressed analytically due to the enormous complexity. Therefore, the conclusions have to be based on above-presented derivations. The only improvement, which was not discussed before, is the use of the elements D_F, C_D and R_D. Mathematical description of this modification is very complicated due to the presence of the non-linearity. The function of D_F, R_F and C_F is to limit high values of the Kalman gain during the

convergence process. As already discussed, SKN containing the low-pass filter only decreases the influence of the eigenvalue ratio - hence, the combination of proposed modifications is important.
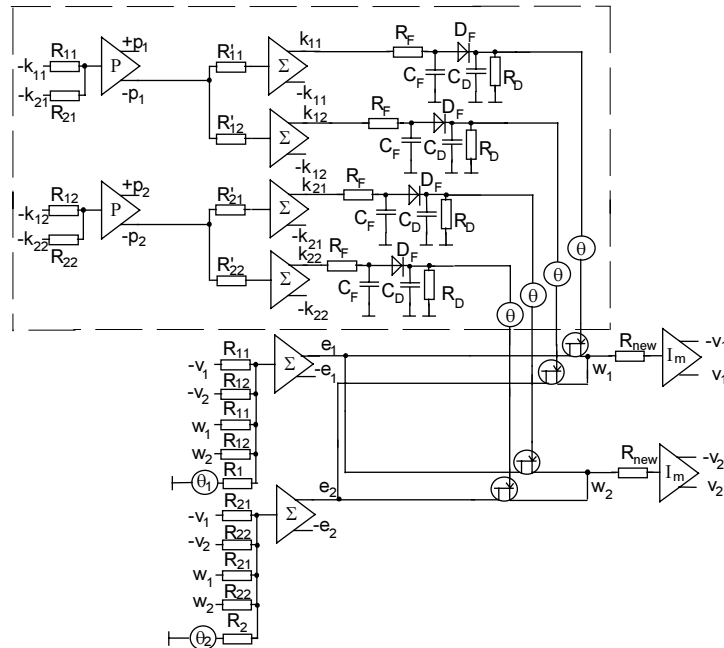

Fig. 2.14: Analog realization of the improved SKN for solving of simultaneous linear equations

Finally, we can conclude that the combined SKN is convenient for the exploitation to the control of adaptive antennas. This conclusion is supported by results of computer simulations.
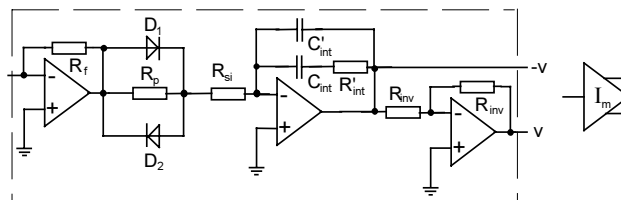

Fig. 2.15: Modified integrator

3 APPLICATION OF ANN IN ADAPTIVE ANTENNA SYSTEMS

In Chapter 1, we have demonstrated the fact that the problem of steering adaptive antenna arrays can be converted to the set of simultaneous linear equations. Real-time iterative solution of these equation sets is then performed by developed ANNs.

We have applied all the developed ANNs to the control of adaptive antennas.

Control of adaptive antennas by original improvements of Wang ANN and Kalman one was simulated and results of computer simulations were compared. The comparison confirmed conclusions of Chapter 2: the control system based on Wang

ANN converged relatively slowly, the control system based on SKN showed higher dependence of the convergence rate on eigenvalue ratio and input signal frequency. Finally, the combined SKN exhibited both high convergence rate and low dependence on the eigenvalue ratio and input-signal frequency. Therefore, this circuit can be found the most suitable for the control of adaptive antennas.
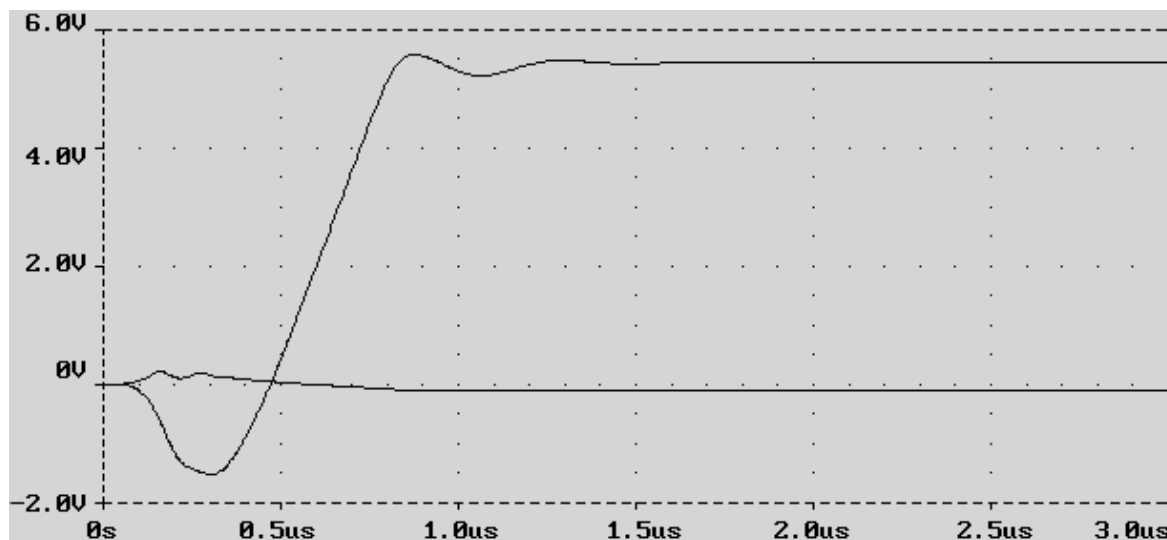

Fig. 2.16: The time course of the vector of solutions of the two-dimensional combined SKN for eigenvalue ratio equal to 70000 in the optimal case

4   CONCLUSIONS

In second chapter, two important types of the analog neural networks (Wang ANN, SKN) were analyzed and discussed. On the basis of the performed analysis, improvements of Wang ANN and SKN were proposed and implemented. Improved ANNs exhibit both high convergence rate and good stability properties, which enable their exploitation in such real time systems as the adaptive antennas are.

First, Wang ANN with the use of the non-linear time constant was presented and mathematically analyzed. At the beginning of the convergence process, the convergence rate is increased using low value of the non-linear time constant, which is later increased in order to prevent unstable state of the ANN. The convergence rate is (compared to the classical Wang ANN) much higher, which confirms the conclusion of the mathematical analysis of this circuit.

Next, the improvement exploiting a parallel connection of a capacitor and the integrating resistor, and the improvement exploiting a serial connection of a resistor and the integrating capacitor were presented and analyzed. The fact that the analysis based on ideal opamps can lead to improper conclusions was confirmed again: in the case of ideal opamps, the analysis leads to the conclusion, that both improved networks exhibit lower convergence rate than the classical Wang ANN. If an output resistor and a limited gain are considered in the summing amplifier, the analysis leads to the opposite conclusion, confirmed also by computer simulations.

The dependence of the convergence rate on the ratio of eigenvalues of the input signal matrix is another important problem, which was not solved by above-mentioned improvements. The unpleasant consequence of this dependence is a long convergence time in the case of a big eigenvalue ratio. This property is undesired in applications, where the high convergence rate is required. The best solution from both older and newly developed approaches in thesis was the application of the modified Kalman filter algorithm. In real conditions, convergence problems of classical Kalman network are similar to those of Wang one, but reached convergence rate is much higher. In order to improve the convergence properties, we can adopt the same improvements as for Wang ANN. Even the results are similar.

An original improvement of the Kalman neural network is exploitation of the low-band filter in the predictor sub-circuit. That way, the signal of the Kalman gain $K(t)$ is filtered in order to reach higher convergence rate. Combining above described improvements, very fast ANN with very low dependence of the convergence rate on the eigenvalue ratio is obtained. It can be concluded, that such neural network can be used also for real time processing in such applications as the adaptive antennas are.

Further, we discussed the use of previously presented analog neural networks in the adaptive antenna systems. We described application of these analog neural networks in the adaptive antenna control systems, including original mathematical analysis of such application of the simplified Kalman network. On the basis of previous conclusions, the modified Kalman neural network with the best convergence properties was applied in the adaptive antenna control system, designed circuit was simulated and results of computer simulations compared with results of computer simulations of the control systems based on the classical Wang ANN and classical SKN. Such comparison confirmed the conclusions – the control system based on the Wang network converged in relatively long convergence times, the control system based on the classical Kalman network showed high dependence of the convergence rate on the ratio of eigenvalues and frequency of the input signal, and the circuit based on the modified Kalman network exhibited both high convergence rate and low dependence of the convergence rate on ratio of eigenvalues and frequency of the input signal. Therefore, this circuit can be considered the most suitable for the control of adaptive antennas.

5 BIBLIOGRAPHY

[1] WIDROW, B., MANTEY, P. E., GRIFFITHS, L. J., GOODE, B. B. Adaptive Antenna Systems. *Proceedings of IEEE.* 1967, vol. 55, no. 12, p. 2143 - 2159.

[2] FROST, O. L. An Algorithm for Linearly Constrained Adaptive Array Processing. *Proceedings of IEEE.* 1972, vol. 60, no. 8, p. 926 - 935.

[3] HOWELLS, P. W. Explorations in Fixed and Adaptive Resolution at GE and SURC. *IEEE Transactions on Antennas and Propagation.* 1976, vol. 24, no. 5, p. 575 - 584.

[4] BOYLE, G., COHN, B., PEDERSON, D. Macro-modeling of Integrated Circuit Operational Amplifiers. *IEEE Journal on Solid - State Circuits.* 1974, vol. 9, no. 6, p. 353 – 364.

[5] POSPÍŠIL, J., DOSTÁL, T. *Electronic Circuits and Systems I.* Brno: Brno University of Technology, 1991 (in Czech).

[6]   RAIDA, Z. Stability of Digital Adaptive Antennas. *PhD thesis*. Brno: Brno University of Technology, 1994 (in Czech).

[7]   RAIDA, Z. Improvement of Convergence Properties of Wang's Neural Network. *Electronics Letters*. 1994, vol. 30, no. 22, p. 1864 - 1866.

[8]   APPLEBAUM, S. P. Adaptive Arrays. *IEEE Transactions on Antennas and Propagation*. 1976, vol. 24, no. 5, p. 585 - 598.

[9]   COMPTON, R. T., Jr. Improved Feedback Loop for Adaptive Arrays. *IEEE Transactions on Aerospace Electronics Systems*. 1980, vol. 16, no. 2., p. 197 – 208.

[10] KLEMES, M. A Practical Method of Obtaining Constant Convergence Rates in LMS Adaptive Arrays. *IEEE Transactions on Antennas and Propagation*. 1986, vol. 34, no. 3, p. 440-446.

[11] KWONG, R. H., JOHNSTON, E. W. A Variable Step Size LMS Algorithm. *IEEE Transactions on Signal Processing*. 1992, vol. 40, no. 7, p. 1633 - 1642.

[12] CICHOCKI, A., UNBEHAUEN, R. *Neural Networks for Optimization and Signal Processing*. Stuttgart: J. Willey&Sons Ltd. & B.G. Teubner, 1993.

[13] WANG, J. Electronic Realization of Recurrent Neural Network for Solving Simultaneous Linear Equations. *Electronics Letters*. 1992, vol. 28, no. 5, p. 493 – 495.

6   SELECTED PUBLICATIONS OF THE AUTHOR

[1]   TOBEŠ, Z. Block Algorithms for the Control of Adaptive Antenna Arrays. *Radioengineering*. 1995, vol. 4, no. 3, p. 1 – 8.

[2]   TOBEŠ, Z., RAIDA, Z. Stability Problems of Wang's Neural Networks. In *Proceedings of the National Conference Radioelektronika '96*. 1996, Brno: Brno University of Technology, p. 366 – 369.

[3]   TOBEŠ, Z., RAIDA, Z. Analog Neural Networks for the Control of Adaptive Antennas. In *Proceedings of the International Symposium on Antennas JINA'96*. 1996, Nice (France): France Telecom, p. 601 – 604.

[4]   TOBEŠ, Z. Application of Neural Networks in Adaptive Antenna Systems. In *Proceedings of the International Conference Neural Networks and Their Application Possibilities*. 1996, Košice (Slovakia): TU Košice, p. 107 – 112.

[5]   TOBEŠ, Z. Stability Problems of Kalman Neural Networks. In *Proceedings of the European Conference on Signal Analysis and Prediction ECSAP 97*. 1997, Prague: CTU Prague, p. 459 – 462.

[6]   TOBEŠ, Z. Modified Hopfield Neural Networks for the Control of Adaptive Antennas. In *Proceedings of the International Conference on Electromagnetics in Advanced Applications*. 1997, Torino (Italy): Polytecnico di Torino, Torino, p. 469 – 472.

[7]   TOBEŠ, Z. Analysis of Stability and Convergence Rate of Analog Neural Networks. In *Proceedings of the 2nd International Student Conference on Electrical Engineering "Poster 98"*. Prague: CTU Prague, p. EEC 44.

[8]   TOBEŠ, Z. An Approach to Obtaining Constant Convergence Rates in Adaptive Antenna Systems. In *Proceedings of the 43rd International Scientific Colloquium*. 1998, Ilmenau (Germany): Technische Universität Ilmenau, p.87 – 92.

[9]   TOBEŠ, Z., RAIDA, Z. Analysis of Recurrent Analog Neural Networks. *Radioengineering*. 1998, vol. 7, no. 2, p. 9 – 14.

[10] TOBEŠ, Z. Ensuring of Equal Convergence Rates of Analog Neural Networks. In *Proceedings of the National Conference Radioelektronika '98*. 1998, Brno: Brno University of Technology, p. 388 – 391.

[11] TOBEŠ, Z., RAIDA, Z. Improvements of Analog Neural Networks Based on Kalman Filter. *Radioengineering*. 2002, vol. 11, no. 1, p. 6 – 13.

[12] TOBEŠ, Z., RAIDA, Z. Use of the Analog Neural Networks in the Adaptive Antenna Control Systems. *Radioengineering*. 2002, vol. 11, no. 3, p. 12 – 17.

BIOGRAPHY

Date of birth: 11.6.1971
Place of birth: Hranice na Moravě
Nationality: Czech
Education:

1985-1989	Secondary Technical School of Jedovnice
1990-1995	Brno University of Technology, Faculty of Electrical Engineering and Computer Science, specialization Electronic and Communication
1995-1998	Brno UT, FEECS, internal doctoral studies at the Institute of Radioelectronics
1995-2000	Masaryk University of Brno, Faculty of Law

Praxis:

9/1989-9/1990	Důl ČSM Stonava, service electrician
10/1998-3/1999	Civil service
4/1999-10/1999	Lachema Brno, specialist for measurement and automation
11/1999-10/2001	TOS Kuřim-OS, programmer and design engineer
11/2001-today	EHSID Steuerungsanlagen GmbH, programmer (Green Card for Germany)

Language knowledge:

English, German, French, Italian, Russian

Research activities:

Adaptive antennas, neural networks, fuzzy logic, digital adaptive algorithms, analog circuits